

INFLUENCE OF GRAPHITE ON THE HARDNESS AND WEAR BEHAVIOR OF AA6061-B₄C COMPOSITE

VPLIV GRAFITA NA TRDOTO IN VEDENJE KOMPOZITA AA6061-B₄C PRI OBRABI

Subramaniam Prabakaran¹, Govindarajulu Chandramohan², Palanisamy Shanmughasundaram³

¹Karpagam University, Department of Mechanical Engineering, Coimbatore-641021, India

²P.S.G. Institute of Technology and Applied Research, Coimbatore-641042, India

³Karpagam University, Department of Automobile Engineering, Coimbatore-641032, India
prabakaran.s@karpagam.com

Prejem rokopisa – received: 2013-09-21; sprejem za objavo – accepted for publication: 2013-12-10

Dry-sliding-wear behavior of AA6061, AA6061-B₄C composite and AA6061-B₄C-Gr hybrid composite was investigated by employing a pin-on-disc wear-test rig. Hardness tests were also carried out. Graphite was used as a solid lubricant since it is a soft, slippery and greyish-black substance. Because of the cleavage (crystal) loose interlamellar coupling, graphite has good lubricating properties. A comparative analysis was made on the hardness and wear behavior of AA6061, AA6061-B₄C composite and AA6061-B₄C-Gr hybrid composite. Boron carbide is known as a robust material having a high hardness. Worn-out surfaces of the wear specimens after the wear tests were examined with a scanning electron microscope to study the morphology of the worn surfaces. Energy dispersive spectroscopy (EDS) was employed to identify the oxides formed on the worn surfaces of the AA6061-B₄C and AA6061-B₄C-Gr composites after the wear test. It was found that a mutual transfer of the material between the wearing Al-alloy and the steel counterface occurred as the load increased. Oxidative wear occurred at low applied loads and a high velocity, whereas delamination and adhesive wear occurred at a high load and high sliding velocity.

Keywords: boron carbide, dry sliding, graphite particles, pin-on-disc, wear resistance

Preiskovano je bilo vedenje AA6061, AA6061-B₄C-kompozita in hibridnega kompozita AA6061-B₄C-Gr pri suhem drsenju z uporabo naprave "pin on disc". Kot trdno mazivo je bil uporabljen grafit, ki je mehka, spolzka in sivo-črna snov. Zaradi cepljive šibke medlamelarne povezave (v kristalu) ima grafit dobre mazalne lastnosti. Izvršene so bile analize primerjave trdote in vedenja pri obrabi AA6061, AA6061-B₄C-kompozita in hibridnega kompozita AA6061-B₄C-Gr. Borov karbid je poznan kot zdržljiv material z veliko trdoto. Po preizkusu obrabe je bila z elektronskim vrstičnim mikroskopom izvršena preiskava morfologije obrabljene površine vzorcev, da bi ugotovili nastale okside na obrabljeni površini kompozitov AA6061-B₄C in AA6061-B₄C-Gr. Ugotovljeno je bilo, da se pri naraščanju obremenitve pojavi vzajemen prenos materiala med Al-zlitino, ki se obrablja, in jeklom. Oksidativna obraba se je pojavila pri majhnih obremenitvah in velikih hitrostih, medtem ko se je obraba zaradi delaminacije in adhezije pojavila pri velikih obremenitvah in velikih hitrostih drsenja.

Ključne besede: borov karbid, suho drsenje, grafitni delci, "pin-on-disc", odpornost proti obrabi

1 INTRODUCTION

Metal-matrix composites have received a lot of commercial attention due to their enhanced mechanical properties, wear resistance and low coefficient of thermal expansion.¹ Metal-matrix composites have many application areas such as automotive and ballistic industries, infrastructure, space and air vehicles, under-water vehicles and deep-ocean equipment. In addition, metal-matrix composites have other advantageous characteristics such as good strength-to-weight ratio, high specific stiffness, high hardness, high plastic-flow strength, good thermal expansion, thermal stability, creep resistance, and good oxidation and corrosion resistance.²

Boron carbide exhibits excellent physical and mechanical properties. Boron carbide is a low-density ceramic with a high hardness and Young's modulus which make it a valuable candidate for engineering applications. Rama Rao and Padmanabhan³ reported that an addition of boron carbide decreases the density of composites and increases the hardness. Gómez et al.⁴ reported that the hardness and strength of composites increased together

with the volume fraction of reinforcement, reaching its maximum value of 10 % B₄C. Wear is a removal of a material from one or both of the two solid surfaces in a solid-state contact. An addition of hard ceramic particles improves the wear resistance of a matrix material. The wear rate is associated with the sliding velocity, normal load, particle size, hardness, particle volume fraction and particle homogeneity.⁵ Jinfeng et al.⁶ observed that with an addition of graphite, the friction coefficient of Al-SiC composites decreases and the wear resistance is significantly increased. Ames and Alpas⁷ reported that Al-Gr composites had a higher wear resistance than Al-SiC composites.

A solid lubricant provides protection from damage during relative movement between the sliding elements and reduces the wear. Miyazaki et al.⁸ analyzed the mechanical behavior of graphite-and-boron-carbide composites made with the hot-pressing method. They reported that the strength of a composite increased with an increase in the boron-carbide content. Many research works were carried out to investigate the sliding-wear behavior of aluminum MMCs reinforced with different

types of reinforcements such as SiC, Al₂O₃ and B₄C. But limited studies have been carried out on hybrid metal-matrix composites.

Shorowordi et al.⁹ studied three aluminium metal-matrix composites containing the reinforcing particles of B₄C, SiC and Al₂O₃ (volume fractions, $\varphi = 0\text{--}20\%$) that were manufactured with the stir-casting method followed by hot extrusion. They reported that the B₄C-reinforced Al-composite seemed to exhibit a better interfacial bonding compared to the other two composites.

Stir casting appears to be the best method for the production of metal-matrix composites compared to the other processing techniques because of its simplicity, allowing an economical large-scale production. The aim of this study is to analyze the influence of graphite particles on the hardness and wear behavior of AA6061-B₄C composites fabricated using a two-stage stir-casting method. The wear tests were carried out by employing a pin-on-disc wear-testing rig. Scanning Electron Microscopy (SEM) was employed to study the microstructures of the composites and the morphologies of the worn surfaces of the composites. Energy Dispersive Spectroscopy (EDS) was used to characterize the Mechanically Mixed Layer (MML) formed on a worn surface during the sliding wear and to elucidate its influences on the wear behavior of the composites.

2 EXPERIMENTATION

2.1 Experimental description

In this study, a two-stage stir-casting method was employed to fabricate AA6061-B₄C and AA6061-B₄C-Gr composites. Brinell hardness testing equipment was employed to measure the hardness of the AA6061 alloy and the composites. The dry-sliding wear behavior of AA6061 and the composites was tested with a pin-on-disc wear-testing rig. Scanning Electron Micro-

scopy (SEM) was employed to study the microstructures and morphologies of the worn surfaces of AA6061, AA6061-B₄C and AA6061-B₄C-Gr composites.

2.2 Specimen preparation

In this study, we used AA6061 as the matrix material, B₄C particles with the average size of 20–50 μm as the reinforcement and graphite particles of 20 μm as the solid lubricant. The composition of AA6061 is presented in **Table 1**. The stir-casting setup is shown in **Figure 1**.

Table 1: Composition of AA6061 (mass fractions, w/%)

Tabela 1: Sestava AA6061 (masni deleži, w/%)

Element	Si	Fe	Cu	Mn	Mg	Cr	Ti	Ca	Al
%	0.359	0.221	0.219	0.032	0.901	0.053	0.141	0.013	Bal

A two-stage stir-casting route was adopted to fabricate the composites. Both B₄C and graphite particulates were preheated at 300 °C in a separate muffle furnace. AA6061 was charged into the crucible and heated up to 650 °C in order to completely melt the aluminium and then the stirring was done at 300 r/min. During the stirring, degassing tablets were added to drive away the entrapped gases from the melt. The stirring was carried out for 3 min. During the stirring, preheated $w = 10\%$ B₄C and 3 % graphite particulates were added. The melt temperature was brought down to 575 °C to reach a semi-solid state. At this stage the stirring was done for 3 min. The composite slurry was again reheated to the temperature of 650 °C and stirred at 300 r/min for 3 min. Finally, the composite slurry was poured into a steel die cavity of 90 mm × 90 mm × 7 mm to solidify. The melting was done in an electric resistance furnace (2 kW – 1 kg capacity). The temperatures were measured with a thermocouple with an accuracy of ± 3 K.

2.2.1 Hardness-test specimens

The poured samples of 1) the AA6061 alloy, 2) composite AA6061-B₄C and 3) AA6061-B₄C-Gr were machined on their four sides to obtain 50 mm squares. All the edges and corners were made blunt/rounded to ensure safety while handling.

2.2.2 SEM analysis (microstructure)

With electric discharge machining, three different samples were machined to rectangular pieces of 10 mm × 20 mm with a thickness of 6 mm. Then these samples were mounted using a heat-conducting, quick-setting epoxy resin. After the mounting each sample was manually polished with a 1200-grade silicon-carbide emery sheet with the help of a diamond paste of 7 μm until achieving a mirror-like finish. The polished surfaces were then etched with a 2 % nitric acid and 98 % alcohol etching solution for 10 s.



Figure 1: Two-stage stir-casting setup

Slika 1: Dvostopenjska naprava za vmešavanje delcev

2.2.3 Wear-analysis specimens

Pin specimens with a width of 6 mm and a height of 30 mm were prepared with EDM (Electric Discharge Machining). The two ends were cut with high flatness accuracy so that the pin face was thoroughly in line with the disc, held perpendicular to the disc surface during the wear test. Moreover, the wear testing equipment had a split-type holder to ensure a proper alignment throughout the test run. Prior to the wear testing, the specimens were polished with an abrasive paper of silicon carbide of grade 600 followed by grade 1000, then cleaned with ethanol and dried.

2.2.4 EDS analysis specimens

The samples prepared for the SEM analysis were also used for the EDS analysis without any modifications.

2.3 Hardness test

The hardness test was performed on AA6061 and the composite specimens of AA6061-B₄C and AA6061-B₄C-Gr using the Brinell hardness testing equipment with a 2.5 mm steel-ball diameter at a load of 1839.4 N. The loading time was 30 s. Three readings were taken for each specimen to eliminate the possibility of segregation and the mean value was considered.

2.4 Microstructure analysis

A scanning electron microscope was employed to study the distribution of boron-carbide and graphite particles in the Al-matrix. The bonding quality between the particulates and the matrix was also studied.

2.5 Dry-sliding wear test

The wear tests were carried out under varying loads of (5, 10, 15 and 20) N at the sliding velocities of 1 m/s and 3 m/s by employing a pin-on-disc wear-testing rig (DUCOM, TR-20LE) with a data-acquisition system shown in **Figure 2**. Each test was conducted for at least 30 min.

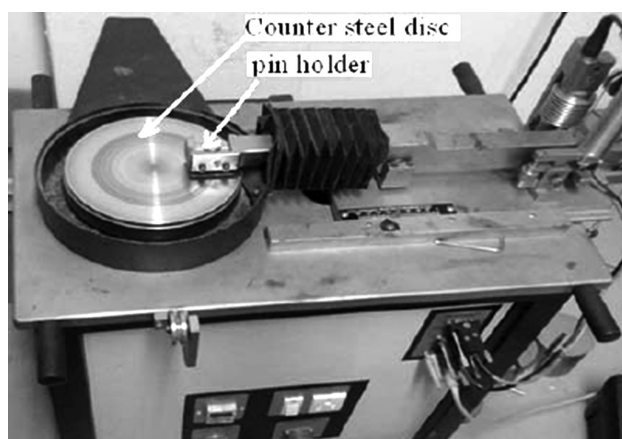


Figure 2: Pin-on-disc wear-testing rig
Slika 2: Naprava "pin on disc" za preizkušanje obrabe

The main parts of the apparatus are a variable-speed electric motor with a steel disc attached to it and a lever arm to which the weight is added. The wear loss of the sample pins was measured in terms of the height loss in microns with the accuracy of 1.0 μm . A track diameter of 100 mm was selected for the analysis. The rotating disc was made of the EN 31 steel having the hardness of 62 HRC. The wear tests were carried out at a room temperature of 30 $^{\circ}\text{C}$ and a relative humidity of 60 % for 30 min, the contact pressure on the disc being 0.14 N/mm² (at 5 N load), 0.28 N/mm² (at 10 N load), 0.42 N/mm² (at 15 N load) and 0.56 N/mm² (at 20 N load). Two samples were tested for each condition. A SEM examination was carried out on the worn surfaces of the specimens in order to understand the wear mechanism under various test conditions.

2.6 Energy Dispersive Spectroscopy (EDS) analysis

An EDS analysis was done on the worn surfaces of the AA6061 alloy and AA6061-B₄C-Gr composite (Jeol) primarily to verify the presence of oxides on the worn surfaces. The data output plots the original spectrum showing the number of X-rays collected at each energy level and mapping the element distributions over the areas of interest.

3 RESULTS AND DISCUSSION

3.1 Microstructural analysis

The microstructure of the AA6061-B₄C-Gr hybrid composite (**Figure 3**) was fabricated with the stir-casting method. It can be seen that the boron-carbide and graphite particles are distributed uniformly, bonding well with the aluminum matrix. The interface between the Al-matrix, boron-carbide and graphite particles is clean allowing a strong interfacial bonding. No agglomeration of the particles was observed in the composite.

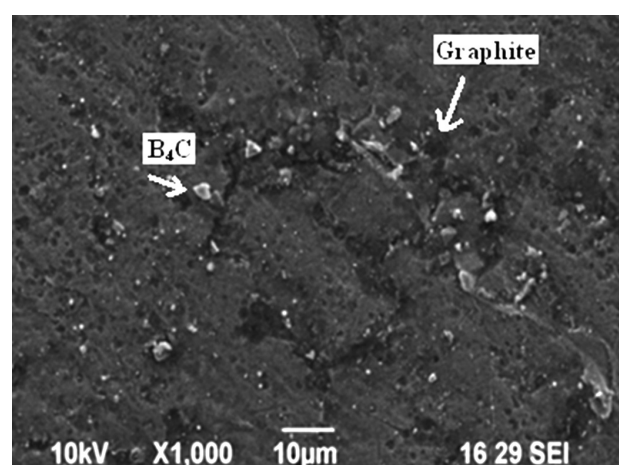


Figure 3: Microstructure of AA6061-B₄C-Gr hybrid composite
Slika 3: Mikrostruktura hibridnega kompozita AA6061-B₄C-Gr

3.2 Hardness analysis

It can be observed from **Figure 4** that the hardness of the Al-matrix increased from 50 BHN to 83 BHN due to the addition of $w = 10\%$ of boron-carbide particles. This reveals an increase in the hardness due to the addition of boron carbide. On the other hand, the hardness of AA6061- B_4C composites decreased from 83 BHN to 66 BHN when graphite particles were incorporated. This can be elucidated with the fact that graphite has a lower hardness than B_4C particles. The hardness of Al-10% B_4C -3% graphite was by about 21% lower than the hardness of the Al-10% B_4C composite. A similar observation was made by Hassan et al.¹⁰

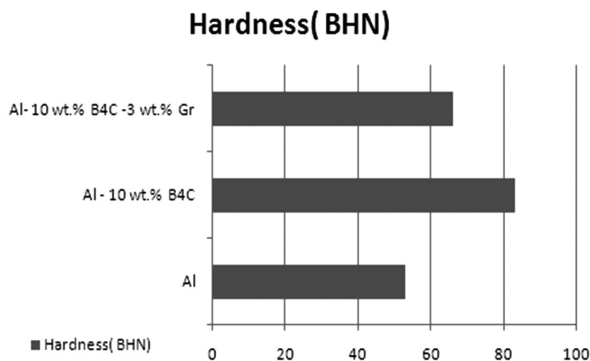


Figure 4: Hardness of AA6061, Al-10% B_4C and Al-10% B_4C -3% Gr (mass fractions, w/w%)

Slika 4: Trdota AA6061, Al-10% B_4C in Al-10% B_4C -3% Gr (masni deleži, w/w%)

3.3 Dry-sliding wear test

Typical curves of the wear loss of matrix AA6061 at the 3 m/s sliding velocity and of hybrid composite AA6061- B_4C -Gr at the sliding velocity of 3 m/s and the constant load of 20 N are presented in **Figures 5 and 6**, respectively. It can be observed that the wear of hybrid

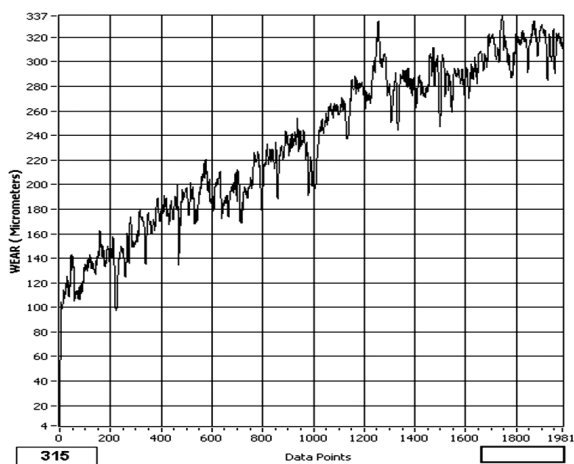


Figure 5: Typical curve of the wear-loss pattern of AA6061 at a load 20 N and 3 m/s sliding velocity for a duration 30 min

Slika 5: Značilna krivulja obrabe AA6061 pri obremenitvi 20 N, hitrosti drsenja 3 m/s in trajanju 30 min

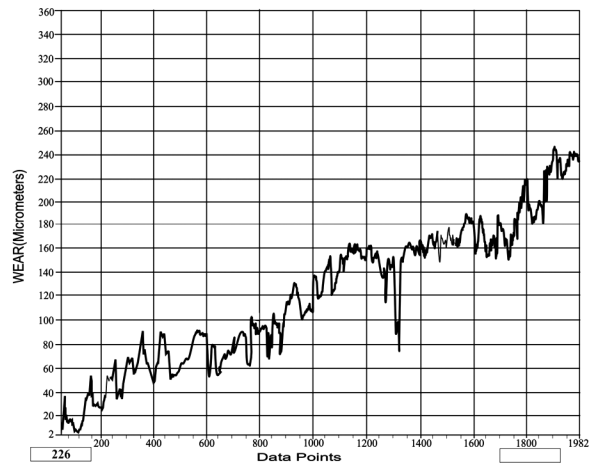


Figure 6: Typical curve of the wear-loss pattern of AA6061- B_4C -Gr at 20 N and 3 m/s sliding velocity for a duration 30 min

Slika 6: Značilna krivulja obrabe AA6061- B_4C -Gr pri obremenitvi 20 N, hitrosti drsenja 3 m/s in trajanju 30 min

composite AA6061- B_4C -Gr is lower by 28% when compared with matrix AA6061. This is due to the presence of the B_4C and graphite particles. This can also be attributed to a better interfacial bonding between Al and the B_4C particles. The volume of the wear debris increases with the increasing load, resulting in a greater loss of the material. The wear resistance of the Al- B_4C composites tends to decrease when the sliding velocity is increased from 1 m/s to 3 m/s at the load of 20 N. In general, a higher sliding velocity generates a higher frictional heat which increases the wear.

It can be observed from **Figures 7 and 8** that the wear loss increased with the increasing load. The volume of the wear debris increases with the increasing load, resulting in a greater loss of the material. The wear resistance of the AA6061- B_4C composites tended to decrease when the sliding velocity was increased from 1 m/s to 3 m/s at the load of 20 N. In general, a higher

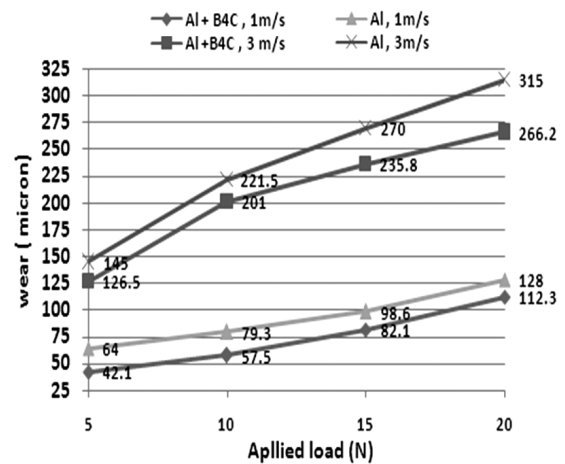


Figure 7: Variation of the wear as a function of normal loads and sliding velocities for AA6061 and AA6061- B_4C composite

Slika 7: Spreminjanje obrabe v odvisnosti od obremenitve in hitrosti drsenja za kompozita AA6061 in AA6061- B_4C

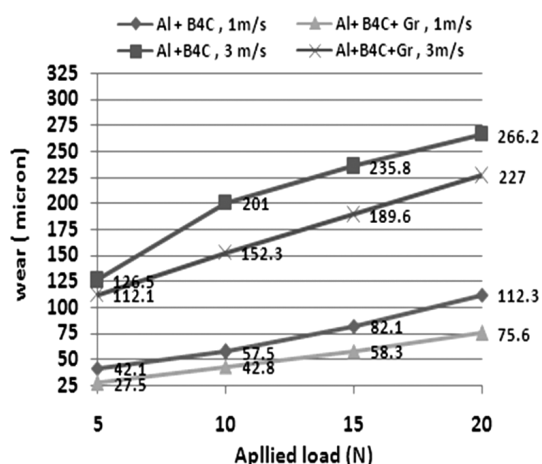


Figure 8: Variation of the wear as a function of normal loads and sliding velocities for the AA6061-B₄C and AA6061-B₄C-Gr composites

Slika 8: Spreminjanje obrabe v odvisnosti od obremenitve in hitrosti drsenja za kompozita AA6061-B₄C in AA6061-B₄C-Gr

sliding velocity generates a higher frictional heat which increases the wear.

Figure 8 shows that the wear loss of AA6061-B₄C is higher than that of the AA6061-B₄C-Gr composite irrespective of the load and speed. This could be due to the soft nature of graphite particles acting as solid lubricants with a layer lattice lamella crystal structure consisting of hexagonal rings forming thin parallel planes (graphenes). Graphenes are bonded to each other with weak van der Waals forces. The layered structure allows a sliding movement of the parallel planes, hence, reducing the frictional forces between the pin and the counter disc. This results in a reduction of the wear of the AA6061-B₄C-Gr composite which is 15 % lower than that of the AA6061-B₄C composite at the 3 m/s sliding velocity and the 20 N load. A similar observation was noticed by Shanmughasundaram et al.¹¹ for AA6061-Gr ($w = 0-7.5$ %) composites.

3.4 Morphology of worn surfaces

Figures 9 and **10** show the wear-track morphology of AA6061 and the AA6061-B₄C composite, respectively, at the normal load of 20 N and the 3 m/s sliding velocity. The worn surface of aluminium with large ploughing grooves is shown. The AA6061 material is much softer than the carbon-steel disc; the asperities on the steel counter face pierce to a larger depth. A larger plastic deformation is seen on the worn surface. The worn surface of the AA6061-B₄C composite (**Figure 10**) shows that the extent of the material removal is not as large as in the case of the AA6061 matrix (**Figure 9**). The wear grooves are smaller along the sliding direction due to the incorporation of boron carbide.

The worn surface of the AA6061-B₄C-Gr composite subjected to the 20 N load at the 1 m/s sliding velocity is shown in **Figure 11**. It shows that the extent of the

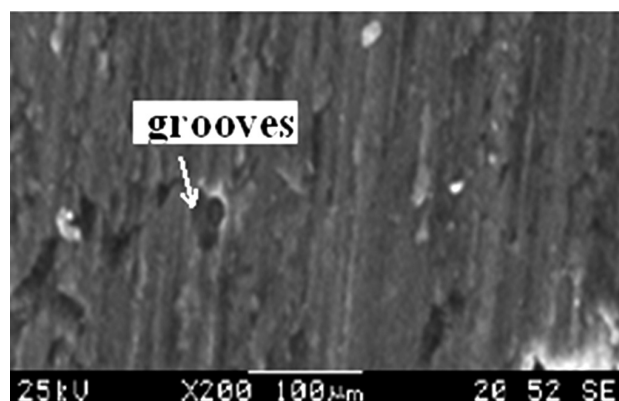


Figure 9: SEM micrograph of the worn surface of AA6061 at the normal load of 20 N and 3 m/s sliding velocity

Slika 9: SEM-posnetek obrabljene površine AA6061 pri obremenitvi 20 N in hitrosti drsenja 3 m/s

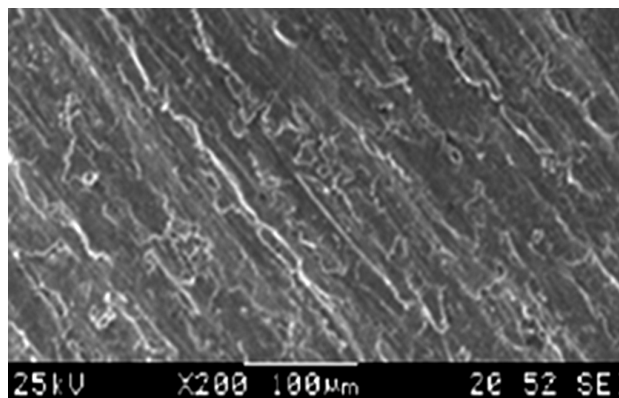


Figure 10: SEM micrograph of the worn surface of the AA6061-B₄C composite at the normal load of 20 N and 3 m/s sliding velocity

Slika 10: SEM-posnetek obrabljene površine AA6061-B₄C kompozita pri obremenitvi 20 N in hitrosti drsenja 3 m/s

material removal is not as large as in the case of the AA6061-B₄C composite. Graphite is a solid lubricant and its particles are soft, slippery, greyish-black, having a layer lattice lamella crystal structure. Its layered structure allows a sliding movement of the parallel



Figure 11: SEM micrograph of the worn surface of the AA6061-B₄C-Gr composite at the normal load of 20 N and 1 m/s sliding velocity

Slika 11: SEM-posnetek obrabljene površine kompozita AA6061-B₄C-Gr pri obremenitvi 20 N in hitrosti drsenja 1 m/s

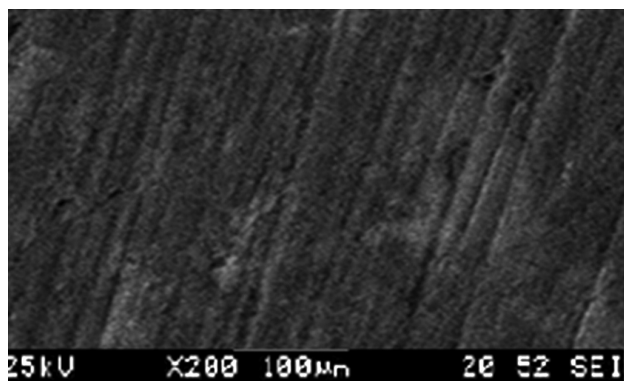


Figure 12: SEM micrograph of the worn surface of the AA6061-B₄C-Gr composite at the normal load of 20 N and 3 m/s sliding velocity

Slika 12: SEM-posnetek obrabljene površine kompozita AA6061-B₄C-Gr pri obremenitvi 20 N in hitrosti drsenja 3 m/s

planes. Hence, it reduces the friction between the pin and the disc, thus, reducing the wear. This observation proves that the wear loss of the hybrid composite of AA6061-B₄C-Gr is lower compared to the AA6061-B₄C composite. The SEM micrograph does not indicate any delamination. The sliding marks (**Figure 12**) obtained at the 3 m/s velocity are relatively higher compared with the low velocity (1 m/s) when viewed at the same magnification. This can be noticed when the sliding velocity increases from 1 m/s to 3 m/s. The morphologies of the worn surfaces gradually change from fine scratches to grooves. This shows that the transition from mild wear to severe wear takes place with an increase in the sliding velocity at a higher load. Generally, aluminium and reinforcement particles react with the oxygen in the air, forming iron oxides during the wear and a Mechanically Mixed Layer (MML) on the worn surface. This oxide film tends to deteriorate at the higher sliding velocity due to a higher frictional heat and increases the wear. It can be concluded that the SEM observation of the worn surfaces of AA6061 and the composites validate the results of the wear loss.

3.5 Energy Dispersive Spectroscopy (EDS) analysis

When the sliding velocity is increased to 3 m/s at the low load (5 N), the surface of the composite pin reacts with the oxygen and forms an oxide layer due to a higher frictional heat. It reduces the direct metallic contact between the sliding surfaces resulting in a lower wear rate of the composite. As can be seen from **Figure 13**, the peak of the oxide which is the main constituent of MML is clearly detected on the worn surface of the composite. It indicates that the oxidative wear is predominant at the low load (5N) and high sliding velocity (3 m/s). Moreover, a negligible amount of oxides was observed on the worn surface of AA6061.

Figure 14 shows the EDAX spectrum of MML for the Al-10 % B₄C-3 % Gr composite when tested at 20 N, 3 m/s. It can be observed that the amount of the oxi-

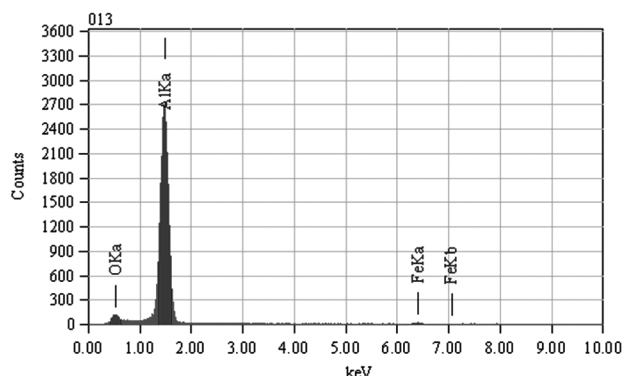


Figure 13: EDAX spectrum of MML for the Al-10 % B₄C-3 % Gr composite tested at 5 N, 3 m/s

Slika 13: EDAX-spekter MML za kompozit z Al-10 % B₄C-3 % Gr, preizkušen pri 5 N in 3 m/s

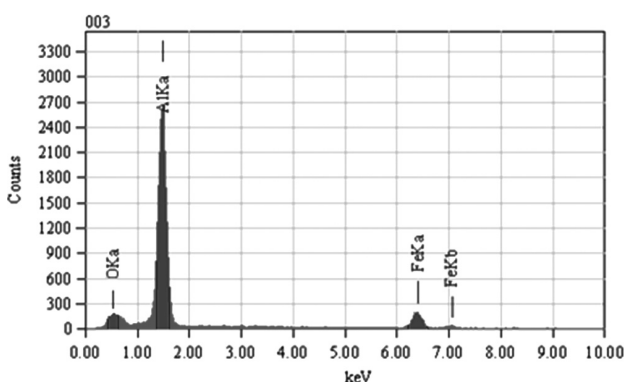


Figure 14: EDAX spectrum of MML for the Al-10 % B₄C-3 % Gr composite tested at 20 N, 3 m/s

Slika 14: EDAX-spekter MML za kompozit z Al-10 % B₄C-3 % Gr, preizkušen pri 20 N in 3 m/s

des present on the worn surface tends to decrease. It can also be noted from **Figure 15** that a considerable amount of iron is transferred from the counter steel disc to the composite pin. However, broken and uneven oxide segments increase the wear. Hence, MML failed to sustain

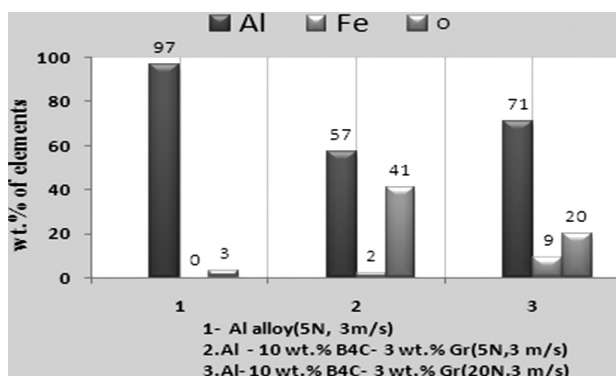


Figure 15: Weight percentage of Al, Fe and oxides as a function of the load and sliding velocity on the worn surface of the Al-10 % B₄C-3 % Gr composite against the counter steel obtained with EDS

Slika 15: Masni deleži Al, Fe in oksidov, ugotovljeni z EDS, v odvisnosti od obremenitve in hitrosti drsenja na obrabljeni površini Al-kompozita z 10 % B₄C in 3 % Gr v paru z jeklom

under the high load and velocity during the sliding. A higher sliding velocity increases the interface temperature and causes a local yielding, thereby the wear mechanism changes into the delamination wear. This behavior is termed as severe wear behavior, in which the material removal occurs at a higher rate. The transition from mild to severe wear is associated with the existence of delamination and adhesion, which are the primary wear mechanisms at the higher load and sliding velocity.

4 CONCLUSIONS

AA6061-B₄C and AA6061-B₄C-Gr composites were successfully fabricated by employing the stir-casting method. A SEM analysis revealed that boron-carbide and graphite particles are distributed uniformly in the aluminium matrix. The AA6061-B₄C composite had a higher hardness compared to AA6061. The wear resistance of the AA6061-B₄C-Gr hybrid composite and Al-B₄C composite increase steadily with the sliding load and velocity. The wear resistance of the AA6061-B₄C-Gr hybrid composite is higher than that of the AA6061-B₄C composite and much higher than that of the AA6061 matrix. The formation of the oxides at the interface plays a significant role in reducing the wear rate. The oxides and reinforcing particles form a mechanically mixed layer (MML) appearing on the worn surface of the composite pin and enhancing the wear resistance. Hence, it can be concluded that graphite particles reduce the wear when included in an aluminium alloy or in an AA6061-B₄C composite.

Acknowledgement

I am grateful to the Faculty of Engineering, Department of Automobile Engineering, Karpagam University, Coimbatore, for providing the facilities for a successful completion of this project.

5 REFERENCES

- ¹ S. Balasivanandha Prabu, L. Karunamoorthy, S. Kathiresan, B. Mohan, *Journal of Materials Processing Technology*, 171 (2006), 268–273
- ² A. A. Cerit, M. B. Karamiş, F. Nair, K. Yildizli, *Tribology in industry*, 30 (2008), 3–4
- ³ S. Rama Rao, G. Padmanabhan, *International Journal of Materials and Biomaterials Applications*, 2 (2012) 3, 15–18
- ⁴ L. Gómez, D. Busquets-Mataix, V. Amigó, M. D. Salvador, *Journal of Composite Materials*, 43 (2009) 9, 987–995
- ⁵ F. Toptan, I. Kerti, L. A. Rocha, *Wear*, 290–291 (2012), 74–85
- ⁶ L. Jinfeng, J. Longtao, W. Gaohui, T. Shoufu, C. Guoqin, *Rare Metal Materials and Engineering*, 38 (2009) 11, 1894–1898
- ⁷ W. Ames, A. T. Alpas, *Metall Mater Trans*, 26A (1995), 85
- ⁸ K. Miyazaki, T. Hagio, K. Kobayashi, *Journal of Materials Science*, 16 (1981) 3, 752–762
- ⁹ K. M. Shorowordi, T. Laoui, A. S. M. A. Haseeb, J. P. Celis, L. Fro-yen, *Technology*, 10 (2003), 738–743
- ¹⁰ A. M. Hassan, G. M. Tashtoush, J. A. Al-Khalil, *Journal of Composite Materials*, 41 (2007) 4, 453–465
- ¹¹ P. Shanmugasundaram, R. Subramanian, *Advances in Materials Science and Engineering*, (2013), article ID 216536